

# Recurrent Mixture Density Network for Spatiotemporal Visual Attention

Loris Bazzani<sup>1</sup>, Hugo Larochelle<sup>2</sup>, Lorenzo Torresani<sup>1</sup>

<sup>1</sup>Department of Computer Science, Dartmouth College, <sup>2</sup>Twitter Cortex  
loris.bazzani@gmail.com, hugo.larochelle@usherbrooke.ca, lt@dartmouth.edu

**Abstract.** The high-dimensional and redundant nature of video have pushed researchers to seek the design of *attentional models* that can dynamically focus computations on the spatiotemporal volumes that are most relevant. Specifically, these models have been used to eliminate or down-weight background pixels that are not important for the task at hand. In order to deal with this problem, we propose an attentional model that learns *where to look* in a video directly from human fixation data. The proposed model leverages deep 3D convolutional features to represent clip segments in videos. This clip-level representation is aggregated over time by a long short-term memory network that connects into a mixture density network model of the likely positions of fixations in each frame. The resulting model is trained end to end using backpropagation. Our experiments show state-of-the-art performance on saliency prediction for videos. Experiments on Hollywood2 and UCF101 also show that the saliency can be used to improve classification accuracy on action recognition tasks.

**Keywords:** Saliency Prediction; Deep Learning; Action Recognition

## 1 Introduction

The last few years have seen tremendous advances in image recognition [1–3] largely thanks to the introduction of large amounts of annotated data [4] and powerful hardware (GPUs), which have enabled the training of deep networks with large number of parameters and great learning capacity. A similar trend is gradually emerging in the domain of video recognition and action classification. As video is much more than a orderless collection of images, methods that perform video analysis by recognition on individual frames are suboptimal. As a result there has been a strong effort in the design of techniques that can model and exploit the temporal information present in a video. Examples include 3D convolutional networks [5, 6], temporal feature fusion at different time resolutions [7, 8] and networks leveraging optical flow [9].

The challenges brought up by video analysis are many. First, videos are very high-dimensional. This effectively constrains the recognition model to be highly efficient in order to be able to handle the large input volume. At the same time, there are obviously strong redundancies present in such data. For example,

the objects or people contained in most videos do not change significantly in appearance over time. On the other hand, if a picture is worth a thousand words, then a video captures the relation between these words through time and therefore tells a complete story [10, 11], which generally cannot be summarized in a single image.

The high-dimensional and redundant signal in video as well as hardware limitations have pushed researchers to seek the design of *attentional models* that can dynamically focus computations on the spatiotemporal volumes that are most relevant, thus reducing the overall computational complexity. Specifically, attentional models have been used to eliminate or down-weight background pixels that are not important for the task at hand, as in image recognition and caption generation [12, 11, 13]. Broadly speaking, attentional models can be split into two categories. The first class is represented by methods that use *soft attention* mechanisms [11, 10, 14, 15]. The second category embodies *hard attentional* methods that completely discard (as opposed to re-weight) information from the input [16–18, 13, 11, 12, 19–21]. All of these methods share the property that the behavior of attention is learned and adapted in the context of its use for a specific task.

In an orthogonal direction, we also find models that learn to attend directly from human gaze scanpaths. In particular, recent work [22–26] has shown that it may be possible to accurately reproduce gazing patterns of human subjects attending tasks in images and videos. This raises the question: can deep networks be trained to reliably predict human scanpath patterns, specifically in such a way that these predictions can be leveraged successfully by a recognition system? In this paper, we explore this question.

We propose an attentional model (see Fig. 1) that learns “where to look” directly from the human scanpath data described in [24, 25]. Our proposed model leverages deep 3D convolutional features [6] to represent each clip of the video. This clip-level representation is aggregated and modeled over time by a Long Short-Term Memory (LSTM) network [27]. The LSTM model is connected to a Mixture Density Network (MDN) [28] that at each frame outputs the parameters of a Gaussian mixture model expressing the saliency map. We refer this model Recurrent Mixture Density Network (RMDN).

The potential applications of automatic saliency map prediction from videos are many. They include attention-based video compression [29], visual attention for robots [30], crowd analysis for video surveillance [31] and salient object detection [32, 33]. In this work we focus on a study of how visual attention may improve action recognition by leveraging the saliency map generated by RMDN for video classification. The idea is akin to soft attention and consists in re-weighting the pixel values of the input video by the estimated saliency map. Despite its simplicity, we show that the combination of features extracted from this modified version of the video and those computed from the original input lead to a significant improvement in action recognition, compared to a model that does not use attention.

The primary contribution of this work is an end-to-end saliency estimation network optimized to reproduce human fixations. The proposed approach offers several advantages: 1) the model can be trained end-to-end without having to engineer features and to use bag-of-feature representations; 2) the model directly uses human fixations to learn the saliency maps, making it very straightforward to train; 3) prediction of the saliency map is very fast (it takes 0.08s per clip); 4) the method outperforms the state-of-the-art [24] in saliency accuracy.

## 2 Related Work

This work falls within the broader literature on models of visual attention. Part of the literature has sought to design models that are *task-agnostic*, i.e. that would reflect the free-viewing properties of attention. These models often rely on the prediction of a saliency map. The task-agnostic saliency methods have been widely explored in the past decades. Researchers have devoted many years to create datasets for this purpose, collecting human fixations and proposing solutions for biologically-plausible saliency estimators (e.g. see [34–36] for recent examples). We refer to [37] for an interesting analysis and comparison of the existing methods. Most of the methods in the literature are focused on extracting features in a bottom-up and/or top-down and use them to estimate the saliency map. In this context, motion features are introduced when extending saliency methods from images to videos [38–40]. However, there is no explicit modeling of the temporal dimension that can capture long-term relations. In fact, the motion features (*e.g.*, optical flow) describe the local-time associations considering only few consecutive frames.

More recently, increased interest and progress has been observed in designing *task-specific* models, particularly in the context of deep neural networks. Such models learn attentional components that are specifically useful for the task at hand. As mentioned previously, these models can be distinguished by how the attentional component extracts information from the input. Soft-attentional components will assign a weight to each attention position and use a weighted average to extract glimpses from images [11, 14, 15] or videos [10]. The advantage of this approach is that it makes it possible to backpropagate through the attentional component and tune it in the context of its use in a deep network. However, this approach does not provide any significant computational benefits to a deep network, since a weight must be computed for each attention position and thus none are entirely ignored. Thus, other work has been directed towards learning hard-attentional models, which explicitly ignore parts of the input [16–18, 13, 11, 12, 19–21]. Unfortunately, since training such models cannot be done simply with backpropagation anymore, they often rely on some form of reinforcement learning and can be much harder to train.

The work mentioned so far attempts to learn attentional models indirectly, i.e. not based on explicit signals as to where a human observer would look. With the accumulation of such datasets however, research has recently attempted to train predictive models directly on such data. In particular, deep neural networks

have been trained to produce saliency maps in this way [41, 14, 42, 32, 43, 44]. One important advantage of using deep networks is that it removes the reliance on feature engineering and therefore requires much fewer assumptions on the principles that govern attention.

To our knowledge, our work distinguishes itself from the aforementioned literature by being the first application of deep neural networks to the prediction of human gaze data in video.

### 3 Proposed Model

We start with a high-level description of our attentional model. We then formalize it in Sec. 3.1, and describe its training in Sec. 3.2. Sec. 3.3 reports how prediction is efficiently carried out at test time. Sec. 3.4 describes the way we exploit the predicted saliency map to improve action recognition.

The proposed RMDN for saliency estimation is depicted in Fig. 1. At time  $t$ , the input of the model is the sequence of  $K = 16$  previous frames (called also clip). The first part of the model (Fig. 1, blue layers above the input clip) consists of a 3D convolutional network that provides a feature representation of the clip. The reason for a clip-based representation rather than a single-frame descriptor is that there is growing evidence [6, 45, 8] that by modeling the temporal information it is possible to obtain improved performances in high-level video analysis tasks, such as action recognition. For our clip representation we use the architecture proposed in [6] (C3D), which has been shown to provide competitive results on video recognition tasks across different datasets. The C3D architecture is defined as: C64-P-C128-P-C256-C256-P-C512-C512-P-C512-C512-P-FC4096-FC4096-softmax, where C is a 3D convolutional layer, P is the pooling layer, FC is a fully-connected layer, and the number specifies the number of kernels of the layer (e.g. C64 has 64 kernels). All convolutional kernels have size  $3 \times 3 \times 3$  (using the time  $\times$  width  $\times$  height notation) and are applied with stride 1. The pooling kernels have size  $2 \times 2 \times 2$  with the exception of the first pooling layer which is  $1 \times 2 \times 2$ .

The convolutional network has access to a limited window of the video since it uses a fixed-size clip of  $K = 16$  frames as input. Therefore it requires a temporal aggregation of the clip-level signal in order to perform video-level decisions. While in [8] simple average pooling of the clips features was shown to yield good action recognition accuracy, our setting demands a more sophisticated temporal modeling optimized to output at each time the attentional fixations based on past and current clip inputs. To this end, we propose to connect the internal representation of the C3D model to a recurrent neural network as shown in Fig. 1 (green module). The aim of the temporal connections of the recurrent neural network is to propagate the clip-level features through time via memory units that can capture long-term dependencies. Our model uses LSTMs [27] as memory block.

The saliency map at each time  $t$  is expressed in terms of a Gaussian Mixture Model (GMM) with  $C$  components. We denote its parameters with  $\{(\mu^c, \pi^c, \Sigma^c)\}_{c=1}^C$ ,

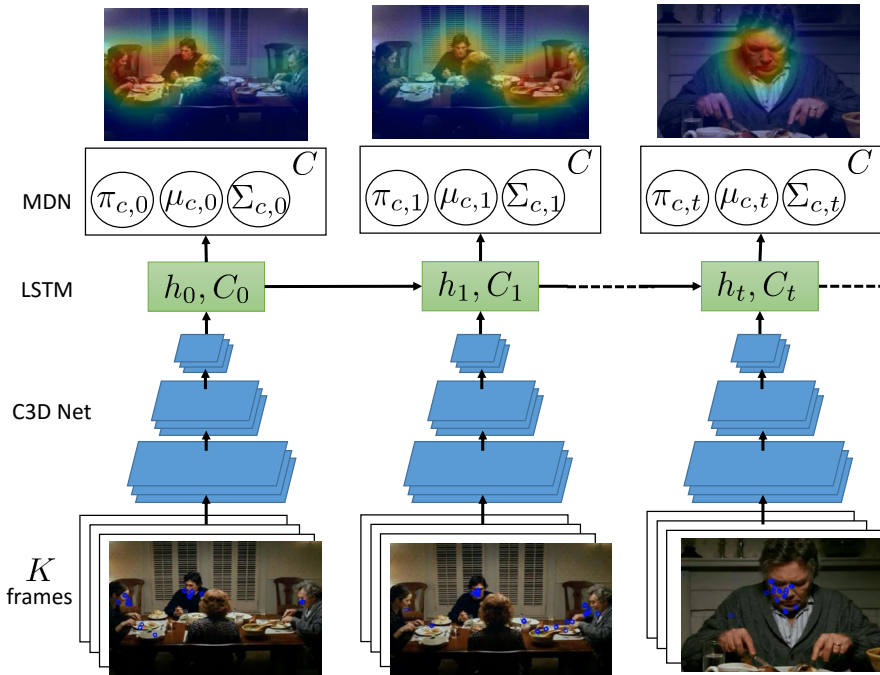


**Fig. 1.** Proposed recurrent mixture density network for saliency prediction. The input clip of  $K$  frames is fed into a 3D convolutional network (in blue), which output becomes the input of a long short-term memory (LSTM) network (in green). Finally, a linear layer project the LSTM representation to the parameters of a Gaussian mixture model, which describes the saliency map.

where  $\mu^c$ ,  $\pi^c$  and  $\Sigma^c$  are the mean, the mixture coefficient and the covariance of the  $c$ -th Gaussian component, respectively. The LSTM is directly outputting these parameters (see details below). The resulting network is known as a Mixture Density Network (MDN) [46, 28].

Since the model is recurrent, there is a direct connection between the inner representation of the LSTM at time  $t$  with the one at time  $t + 1$ . This enforces temporal consistency between the saliency maps at adjacent times.

### 3.1 Formalization of the Model

Let  $\mathcal{D} = \{(\mathbf{v}_i, \mathbf{a}_i)\}_{i=1}^N$  be a dataset of human fixations, where  $\mathbf{v}_i = (\mathbf{c}_t)_{t=1}^{T_i}$  is a video consisting of  $T_i$  temporal overlapping clips  $\mathbf{c}_t$  (i.e., sampled with stride 1) and  $\mathbf{a}_i$  is the set of ground-truth fixations for the  $i$ -th video. Since we use C3D to represent each clip,  $\mathbf{c}_t$  has a fixed length of  $K = 16$  frames. Note that  $T_i$  is equal to the length of the  $i$ -th video minus  $K$ , since we extract clips with a temporal stride of 1 frame. The fixations  $\mathbf{a}_i \in \mathbb{R}^{2 \times A_i}$  are a set of  $(x, y)$  image positions which are normalized to  $[0, 1]$  in order to deal with videos of different resolutions. In practice, the number of fixations per frame  $A_i$  is variable, but in the experiments we control it by subsampling to obtain a fixed-size set for each frame.

Let  $\mathbf{x}_t = \text{C3D}(\mathbf{c}_t)$  be the internal representation of C3D for an input clip  $\mathbf{c}_t$ . In our model we use the last convolutional layer, before the fully-connected

layers. We choose a convolutional layer instead of a fully-connected layer because the latter discards spatial information, which is crucial to estimate a saliency map over the entire image.

The LSTM network [27] is defined as follows:

$$f_t = \sigma(W_f \cdot [h_{t-1}, \mathbf{x}_t] + b_f), \quad i_t = \sigma(W_i \cdot [h_{t-1}, \mathbf{x}_t] + b_i) \quad (1)$$

$$o_t = \sigma(W_o \cdot [h_{t-1}, \mathbf{x}_t] + b_o), \quad \tilde{C}_t = \tanh(W_C \cdot [h_{t-1}, \mathbf{x}_t] + b_C) \quad (2)$$

$$C_t = f_t * C_{t-1} + i_t * \tilde{C}_t, \quad h_t = o_t * \tanh(C_t) \quad (3)$$

where  $f_t$ ,  $i_t$ ,  $o_t$ ,  $C_t$  and  $h_t$  are the forget gate, the input gate, the output gate, the memory cell, and the hidden representation, respectively. The parameters to learn during the training phase are  $W_z$  and  $b_z$  where  $z \in \{f, i, o, C\}$ .

The MDN [46, 28] takes its inputs from the hidden representation of the LSTM network. Since the output space is 2D (the space of image locations), we can reparametrize the model as  $\{(\mu_t^c, \pi_t^c, \sigma_t^c, \rho_t^c)\}_{c=1}^C$ , where  $\mu_t^c$ ,  $\pi_t^c$ ,  $\sigma_t^c$  and  $\rho_t^c$  are the 2D mean position, the weight, the 2D variance and the correlation of the  $c$ -th Gaussian component, respectively. The MDN is therefore defined as follows:

$$y_t = \{(\tilde{\mu}_t^c, \tilde{\pi}_t^c, \tilde{\sigma}_t^c, \tilde{\rho}_t^c)\}_{c=1}^C = W_y \cdot h_t + b_y \quad (4)$$

where  $W_y$  and  $b_y$  are the parameters of the linear layer and  $h_t$  is the hidden representation of the LSTM network.

The parameters of the GMM in Eq. 4 must be renormalized as follows in order to obtain a valid probability distribution:

$$\mu_t^c = \tilde{\mu}_t^c, \quad \pi_t^c = \frac{\exp(\tilde{\pi}_t^c)}{\sum_{i=1}^C \exp(\tilde{\pi}_t^i)}, \quad (5)$$

$$\sigma_t^c = \exp(\tilde{\sigma}_t^c), \quad \rho_t^c = \tanh(\tilde{\rho}_t^c) \quad (6)$$

The composition of the LSTM and the MDN results in the RMDN.

In the next section, we will describe how end-to-end training of the full network is performed.

## 3.2 Training

The proposed model can be trained end-to-end by optimizing the log-likelihood of the training ground truth fixations  $\mathbf{a}_i$  under the GMM. The loss function for the  $i$ -th video  $\mathbf{v}_i$  is defined as the negative log-likelihood of the fixations under the GMM as follows:

$$L(\mathbf{v}_i, \mathbf{a}_i) = \sum_{t=1}^{T_i} -\log \left( \sum_{c=1}^C \pi_t^c \mathcal{N}(\mathbf{a}_i | \mu_t^c, \sigma_t^c, \rho_t^c) \right) \quad (7)$$

where  $\mathcal{N}$  is the Gaussian distribution. Note that the parameters of the Gaussian components are also dependent on the input video  $\mathbf{v}_i$ , but we do not make this explicit in the equation in order to keep notation simple.

The RMDN can be obtained by optimizing the log-likelihood using backpropagation, since it is a composition of continuous functions (e.g. linear transformations and element-wise non-linearities) for which we can compute the gradients. In particular, we refer to [46] for the derivation of the gradients for the MDN using the loss function of Eq. 7. In practice, we freeze the layers of the C3D network to the values pretrained in [6] for action recognition. This implies that the low-level representation  $\mathbf{x}_t$  is fixed. We jointly train the LSTM and MDN from randomly initialized parameters.

### 3.3 Prediction

The inference stage is straightforward by following the equations of Sec. 3.1. At a given time  $t$ , the clip from time  $t - K + 1$  to  $t$  is fed into the C3D network to produce the representation  $\mathbf{x}_t$ . This vector is passed to the LSTM whose hidden representation is passed to the MDN, which outputs the GMM parameters. In order to generate the final saliency map, we compute the probability of each pixel position under the GMM model. We normalize the probability map to sum up to 1 over the image pixels in order to produce a normalized saliency map.

### 3.4 Saliency for Action Classification

As mentioned in the introduction, we propose to use the estimated saliency for video classification. We generate a modified version of the video by using a soft-attention mechanism that weights each pixel value by the estimated saliency at that position. This operation effectively down-weights regions that are deemed not salient. The intuition is that then the classifier will be able to focus on the parts of the frame which are most relevant without being distracted by the non-salient regions (see examples in Fig. 2).

The proposed model for recognition is presented in Fig. 2. At each time  $t$ , we extract two representations: the context branch is given by the C3D representation of the original clip, while the soft attentional branch is given by the C3D representation of the input clip weighted by the saliency map. The rationale is that the context branch considers the global evolution of the activity in the video while the soft attentional branch is focused on the most-salient local evolution of the activity. The two representations are then concatenated at the clip level and max-pooled over the video to obtain the final video-level descriptor. This video-level representation is then used as input to train the video classifier which is a linear SVM in our experiments.

In our experiments, we also evaluated the option of weighting the convolutional feature map  $\mathbf{x}_t$  instead of the input, as for example done in [47]. However, we will see that soft-masking the input gives higher accuracy, probably because applying C3D’s non-linear transformation after the soft-weighting produces a representation that is less redundant with the original (non-masked) C3D representation.

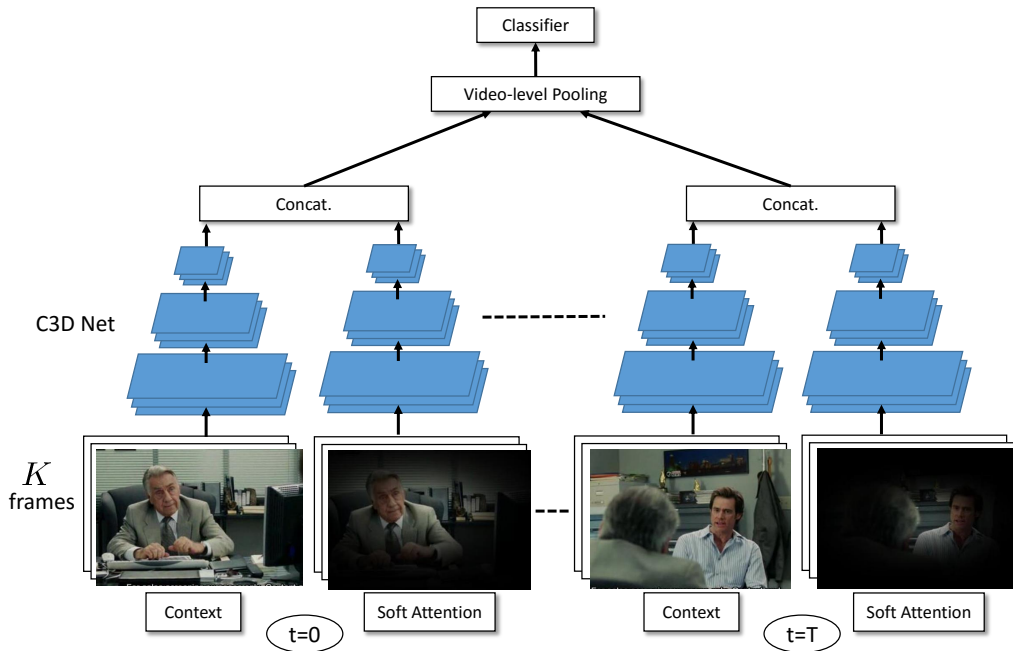


**Fig. 2.** Model for action recognition. The original clip of  $K$  frames is fed into a 3D convolutional network. The same clip is then weighted by the predicted saliency map estimated by our RMDN and then fed into the 3D convolutional network. The final clip-level representation is then concatenated. All the clips of a video are merged using pooling and then a linear classifier can be trained.

## 4 Experiments

In this section, we validate the proposed method for both saliency prediction and action recognition on two challenging datasets: Hollywood2 [48] and UCF101 [49]. We describe the implementation details in Section 4.1. Section 4.2 reports a quantitative analysis for the task of saliency prediction. Section 4.3 shows the results for the action recognition task in two scenarios: 1) using the same dataset which was used to train the saliency predictor and 2) applying the pretrained model to a never-seen dataset and completely different set of actions. The qualitative results of our work can be watched at [https://youtu.be/aX0wc17nx\\_s](https://youtu.be/aX0wc17nx_s).

### 4.1 Implementation Details

We used the pretrained C3D network [6] as feature representation which is the input of the LSTM network. The convolutional layer before the fully-connected layers is used for saliency prediction, while the last fully-connected layer before the softmax is used for classification, since [6] showed to obtain the best performance.

The training of the RMDN is performed using RMSprop with adaptive learning rate and gradient clipping. We start from a learning rate of 0.0003 and after 8 epochs it is reduced at each epoch with a decay factor of 0.95. The gradient is clipped with a threshold of 20. Dropout with a ratio of 0.5 is applied only on the

hidden layer of the LSTM network before the MDN. We trained for 40 epochs, but training is stopped if there is no significative improvement of the loss. During training, temporal data augmentation is performed by clipping the videos to shorter videos of length 65 frames (which corresponds to 50 C3D descriptors since it needs a buffer of 16 frames for the first descriptor). The number of components of the GMM  $C$  is fixed to 20 for all the experiments. All the experiments were carried out using an NVIDIA Tesla K40 card.

After extracting the saliency maps and the feature representations on GPU, our recognition experiments were performed on CPU using a linear SVM. In order to compute the video-level representation, we performed max pooling of the clip-level representations of the video. For all the experiments, we used 20% of the training data as validation set to find the regularization parameter of the SVM. We searched the parameter space on a grid between  $10^{-9}$  to  $10^3$  with a step of  $10^{\frac{1}{2}}$ . Finally, we retrain the SVM on all the training set (including the validation set) using the best cross-validated parameter.

## 4.2 Saliency Prediction

The proposed model is trained using real human fixation data. For this task, few datasets provide both human fixations and class labels (for the action recognition dataset in the next section). Therefore, we used the Hollywood2 dataset that was augmented with eye tracking data in [24]. We follow the same evaluation protocol (*i.e.*, same splits) of [24] and their same validation procedure to compute the final results and compare with it. [24] proposes to generate the saliency maps from a binary fixation map by convolving an isotropic Gaussian filter of size  $\sigma = 1.5$  and  $3.0$  and then adding a uniform distribution with parameter  $p = 0.25$  and  $0.5$ . These two parameters are cross-validated in a separated validation set consisting of 20% of the training set<sup>1</sup>.

In order to evaluate the methods, we used popular metrics proposed by the literature of saliency map prediction for still images [50, 34], such as Area Under the ROC Curve (AUC), Normalized Scanpath Saliency (NSS), linear Correlation Coefficient (CC) and the Similarity score (S). We refer to [50, 34] for their detailed description.

Table 1 shows a set of experiments which aim at evaluating different variants of the proposed model. The first comparison between the Trained Central Bias (TCB) baseline and LSTM shows the value of training a saliency map predictor that leverages temporal information. The TCB is a single GMM that is replicated over all the frames and trained on all the fixations, discarding completely the temporal information and using the same saliency map for each testing frame. This experiment shows that LSTM (with the same number of fixations) always outperforms significantly the TCB.

The second set of comparisons in Table 1 is focused on: 1) the impact of using LSTM hidden units as opposed to regular RNN units (third and fourth

---

<sup>1</sup> Because [24] does not provide the validation set, we used 80% of the training set for actual training and then 20% of it for validation.

row) and 2) the number of fixations per frame used for training (fourth and fifth row). These experiments show that the LSTM (fourth row) is better than an RNN (third row) in terms of AUC and NSS, but in order to have better CC and Sim we need to use more fixations per frame (fifth row). This is intuitive, because LSTM has many more parameters than the RNN, therefore it needs more training data to be trained properly. In fact, LSTM outperforms RNN when using more fixations (fifth row).

The final experiment in Table 1 (last row) uses the full training set of [24] instead of just the 80%. In this experiment we do not perform cross-validation, because the validation set is in the training set now. We used the hyper-parameters selected by the cross-validation of the experiment in the fourth row. This results is our best obtained result for saliency prediction reported in our work and it is the model we used in all the experiments that follow.

We also carried out a few side experiments and discovered that: using the fully-connected features of C3D instead of the convolutional representation gives results that are at least 1.5% lower in terms of AUC. We also experimented with deep LSTMs, but we obtained an insignificant improvement of performance. For this reason and also because deep LSTMs have more parameters and are more computationally expensive to train, we preferred to use a shallow LSTM.

**Table 1.** Saliency prediction results in terms of AUC, NSS, CC and Similarity for different models on Hollywood2 dataset.

Model	Net(#units)	Fix. per frame	AUC	NSS	CC	Sim
Trained Central Bias	–	150	0.8725	1.7646	0.5297	0.4812
RMDN	RNN(128)	80	0.8745	1.9505	0.5495	0.4962
RMDN	LSTM(128)	80	0.8866	2.0155	0.4606	0.4219
RMDN	LSTM(256)	150	0.8986	2.5169	0.6007	0.5278
RMDN full	LSTM(256)	150	<b>0.9037</b>	<b>2.6455</b>	<b>0.6129</b>	<b>0.5349</b>

The proposed method is also compared to state-of-the-art methods for saliency prediction from videos. Table 2 shows the best methods reported by the extensive analysis done in [24] as well as our best result.

The table reports some useful baselines, such as the central bias and the human accuracy for the task. The table also contrasts the use of static features, motion features and their combination. The last row of the right table is showing the results obtained by our method. It is interesting to see that the results obtained with a single type of features (static or motion) have an AUC lower than 0.75, which is even lower than the one obtained by the central bias (0.84). Moreover, the combination reaches the best results only when the central bias is combined with the experiment with engineered features (SF+MF+CB). On the other hand, our method outperforms all the methods evaluated in [24] by a large margin and our results are very close to the human performance (only 3.2% of difference). Apart being the best method in Table 2, our method has

several advantages: 1) it does not include any tedious feature engineering, 2) we perform end-to-end training of the proposed network, 3) human bias can be learned directly from the data.

Our method is also potentially much faster, as the baselines in Table 2 depend on features that are usually computationally expensive to extract. Even though we cannot directly compare with those methods in terms of computational performance, we can report the numbers for our method. The proposed method takes 0.08s per clip for inference on GPU which is divided in 0.07s for C3D and 0.01s for the RMDN.

**Table 2.** Saliency prediction comparison against the state-of-the-art on the Hollywood2 dataset. The top-3 best results for each set are taken from [24]

Set	Model	AUC	Set	Model	AUC
Baselines	Uniform	0.500	MF = Motion Features [24]	Flow magnitude	0.626
	Central Bias (CB)	0.840		Flow bimodality	0.637
	Human	<b>0.936</b>		HOG-MBH det.	0.743
SF = Static Features	Color features [35]	0.644	Combo [24]	SF [35]	0.789
	Saliency map [51]	0.702		SF+MF	0.812
	Horizon det. [51]	0.741		SF+MF+CB	0.871
			Our Method	<b>RMDN</b>	<b>0.904</b>

### 4.3 Action Recognition

In order to show how saliency can be used for action recognition we carried out a set of experiments covering two scenarios: 1) using the same dataset on which the saliency predictor was trained (Hollywood2) and 2) using a never seen dataset with a different set of actions (UCF101).

The results on Hollywood2 are reported in terms of mean Average Precision (mAP) as in [24]. Table 3 shows an analysis of 1) the impact of using different feature representations as well as 2) the effect of the saliency map. The first column shows the two features we tested, as in [6]: CONV5 and FC6 correspond to the fifth convolutional and first fully-connected representation of C3D, respectively. The second column (or experiment (1)) reports the results using only the original video (referred to as context in Fig. 2). The third column and fourth column are the ground truth soft attention in Fig. 2 and its concatenation with the context (experiment (3)), respectively. The last two columns represent the same experiment, but in this case we use the saliency maps predicted by our model.

The two rows differ also in the way that the saliency map is used. In the experiment of the second row (CONV5), we multiply the convolutional layer by the saliency map weighting. In other words, the saliency acts directly on the

feature representation, similarly to [47]. Finally, the experiment in the third row is using exactly the model presented in Sec. 3.4.

Table 3 shows that the performance of using CONV5 and FC6 are very close when considering the original video (experiment (1)) and the ground truth saliency (experiment (2)). However, the concatenation (experiment (3)) is effective only using the proposed method. This experiment shows that weighting the input video and re-extracting the features better diversifies the feature representation. Finally, we can notice from Table 3 that the same behavior is obtained when using the predicted saliency (experiment (4) and (5)). In addition, it is surprising to notice that the difference in the results with the predicted saliency (experiment (5)) and ground truth one (experiment (3)) is negligible (only 0.27%).

**Table 3.** Recognition results in terms of mAP on the Hollywood2 dataset. Analysis of different ways to use the saliency map and comparison between using the ground truth saliency vs. the predicted one.

Saliency	–	Ground Truth		Predicted	
Input	(1) Original	(2) Weighted	(3) Concat. (1, 2)	(4) Weighted	(5) Concat. (1, 4)
CONV5	46.08%	40.76%	45.62%	N/A	N/A
FC6	47.00%	41.78%	55.12%	39.00%	54.85%

Table 4 compares our results with the methods presented in [24]. As we did before, we separate between experiments which use the ground truth saliency and the ones that use the predicted one. The results of Table 4 shows that the performance our method (third and sixth column) is around 2% lower than [24]. However this is most likely explained by the differences in the type of video classification method used, and not by the differences in saliency map prediction methods. Indeed, we already established in Table 2 that our proposed saliency map predictor is much better than the one proposed in [24]. On the other hand, [24] uses a combination of many different features and a kernel chi-square SVM, while our method uses C3D features with a simple linear SVM classifier. Adding more non-linearities, especially for the concatenation experiment, would probably help, though we consider the experimentation with more types of video classifiers as being out of the scope of this paper.

Finally, we perform an experiment to assess the generalization abilities of the learned saliency model to a different dataset, with classes and videos that have not been seen during its training. To this end, we used the attentional model trained on the Hollywood2 dataset to extract saliency maps on the UCF101 dataset. Table 5 reports the recognition results in terms of accuracy on UCF101 using the evaluation protocol and splits in [49]. The proposed method (C3D + RMDN, seventh row) corresponds to the concatenation of the original C3D descriptor and the C3D descriptor with the input weighted by the saliency map, as was done in the Hollywood2 experiments. We compare our method with the

**Table 4.** Recognition results in terms of mAP for the Hollywood2 dataset. The proposed method is compared to the approaches reported in [24].

Class	Ground Truth		Predicted		
	[24]	<b>RMDN (our)</b>	Central Bias	[24]	<b>RMDN (our)</b>
AnswerPhone	28.1%	21.8%	23.3%	23.7%	29.8%
DriveCar	94.8%	89.2%	92.4%	92.8%	91.6%
Eat	67.3%	59.4%	58.6%	70.0%	49.1%
FightPerson	80.6%	80.9%	76.3%	76.1%	79.2%
GetOutCar	55.1%	78.0%	49.6%	54.9%	76.9%
HandShake	27.6%	58.6%	26.5%	27.9%	47.0%
HugPerson	37.8%	27.5%	34.6%	39.5%	37.9%
Kiss	66.4%	52.2%	62.1%	61.3%	51.0%
Run	85.7%	85.5%	77.8%	82.2%	83.2%
SitDown	62.5%	31.8%	62.1%	69.0%	31.4%
SitUp	30.7%	38.0%	20.9%	29.7%	39.7%
StandUp	58.2%	37.8%	61.3%	63.9%	41.3%
Mean	57.9%	55.1%	53.7%	57.6%	54.8%

results using the C3D descriptor only (sixth row) and other state-of-the-art methods reported in [6] (second row through fifth row). The C3D network itself is already outperforming all other methods. Then, we obtain an improvement of 1.1% when using the saliency maps generated by our RMDN (seventh row). This is an impressive result since the RMDN was trained on the fairly small Hollywood2 dataset.

**Table 5.** Recognition results in terms of accuracy for the UCF101 dataset.

Method	Accuracy
Imagenet + linear SVM	68.8%
iDT [52] + BoW + linear SVM	76.2%
Spatial stream network [9]	72.6%
LSTM composite model [45]	75.8%
C3D + linear SVM	80.4%
C3D + RMDN + linear SVM	81.5%

## 5 Conclusions

In this paper, we proposed a recurrent mixture density network for visual attention prediction on spatiotemporal data. We showed that our model outperforms state-of-the-art methods for saliency prediction in videos. Predicted saliency maps generated by our model have also been applied to the problem of action

recognition in a very simple way, proving that saliency can enrich the original representation. The overhead to estimate the parameters of the saliency map is very small: only 0.01s which is added to 0.07s for feature extraction.

As future work, we plan to close the gap between the RMDN and our approach to action recognition with a joint network. The idea is to have as output of the model both the saliency map and the class of the action. This can be combined with the idea of using the saliency map estimated at the previous time to weight the input for the current time. Putting together these two ideas in an end-to-end network would result in a joint model for saliency prediction and action recognition.

**Acknowledgments.** We thank Du Tran for helpful discussion about the code of the C3D network and its usage. We also thank Stefan Mathe for helping understanding the format of the eyetracking data and reproducing the experimental protocol on the Hollywood2 dataset. This work was funded in part by NSF award CNS-1205521. We gratefully acknowledge NVIDIA for the donation of GPUs used for portions of this work.

## References

1. Krizhevsky, A., Sutskever, I., Hinton, G.E.: Imagenet classification with deep convolutional neural networks. In: NIPS. (2012) 1097–1105
2. Szegedy, C., Liu, W., Jia, Y., Sermanet, P., Reed, S., Anguelov, D., Erhan, D., Vanhoucke, V., Rabinovich, A.: Going deeper with convolutions. (2015)
3. Girshick, R., Donahue, J., Darrell, T., Malik, J.: Rich feature hierarchies for accurate object detection and semantic segmentation. In: IEEE CVPR. (2014)
4. Russakovsky, O., Deng, J., Su, H., Krause, J., Satheesh, S., Ma, S., Huang, Z., Karpathy, A., Khosla, A., Bernstein, M., Berg, A.C., Fei-Fei, L.: ImageNet Large Scale Visual Recognition Challenge. *International Journal of Computer Vision (IJCV)* **115**(3) (2015) 211–252
5. Ji, S., Xu, W., Yang, M., Yu, K.: 3d convolutional neural networks for human action recognition. *Pattern Analysis and Machine Intelligence, IEEE Transactions on* **35**(1) (2013) 221–231
6. Tran, D., Bourdev, L., Fergus, R., Torresani, L., Paluri, M.: Learning spatiotemporal features with 3d convolutional networks. (2015) 4489–4497
7. Karpathy, A., Toderici, G., Shetty, S., Leung, T., Sukthankar, R., Fei-Fei, L.: Large-scale video classification with convolutional neural networks. In: CVPR. (2014)
8. Yue-Hei Ng, J., Hausknecht, M., Vijayanarasimhan, S., Vinyals, O., Monga, R., Toderici, G.: Beyond short snippets: Deep networks for video classification. (2015) 4694–4702
9. Simonyan, K., Zisserman, A.: Two-stream convolutional networks for action recognition in videos. In: *Advances in Neural Information Processing Systems*. (2014) 568–576
10. Yao, L., Torabi, A., Cho, K., Ballas, N., Pal, C., Larochelle, H., Courville, A.: Describing Videos by Exploiting Temporal Structure. In: *IEEE International Conference on Computer Vision (ICCV)*. (2015) 4507–4515
11. Xu, K., Ba, J., Kiros, R., Cho, K., Courville, A., Salakhudinov, R., Zemel, R., Bengio, Y.: Show, attend and tell: Neural image caption generation with visual attention. (2015) 2048–2057
12. Sermanet, P., Frome, A., Real, E.: Attention for fine-grained categorization. *CoRR abs/1412.7054* (2014)
13. Mnih, V., Heess, N., Graves, A., et al.: Recurrent models of visual attention. In: *Advances in Neural Information Processing Systems*. (2014) 2204–2212
14. Kümmerer, M., Theis, L., Bethge, M.: Deep gaze I: boosting saliency prediction with feature maps trained on imagenet. (2015)
15. Gregor, K., Danihelka, I., Graves, A., Rezende, D., Wierstra, D.: Draw: A recurrent neural network for image generation. (2015) 1462–1471
16. Larochelle, H., Hinton, G.E.: Learning to combine foveal glimpses with a third-order Boltzmann machine. In: *Advances in Neural Information Processing Systems 23 (NIPS 2010)*, Vancouver, Canada (2010) 1243–1251
17. Bazzani, L., de Freitas, N., Larochelle, H., Murino, V., Ting, J.A.: Learning attentional policies for object tracking and recognition in video with deep networks. In Getoor, L., Scheffer, T., eds.: *Proceedings of the 28th International Conference on Machine Learning (ICML-11)*. ICML '11, New York, NY, USA, ACM (June 2011) 937–944
18. Denil, M., Bazzani, L., Larochelle, H., de Freitas, N.: Learning where to attend with deep architectures for image tracking. *Neural Computation* (2012)

19. Ba, J., Mnih, V., Kavukcuoglu, K.: Multiple object recognition with visual attention. (2015)
20. Yoo, D., Park, S., Lee, J.Y., Paek, A.S., So Kweon, I.: Attentionnet: Aggregating weak directions for accurate object detection. In: The IEEE International Conference on Computer Vision (ICCV). (December 2015)
21. Zheng, Y., Zhang, Y.J., Larochelle, H.: A Neural Autoregressive Approach to Attention-based Recognition. *International Journal of Computer Vision* **113**(1) (2015) 67–79
22. Mauthner, T., Possegger, H., Waltner, G., Bischof, H.: Encoding based saliency detection for videos and images. In: The IEEE Conference on Computer Vision and Pattern Recognition (CVPR). (June 2015)
23. Hossein Khatoonabadi, S., Vasconcelos, N., Bajic, I.V., Shan, Y.: How many bits does it take for a stimulus to be salient? In: The IEEE Conference on Computer Vision and Pattern Recognition (CVPR). (June 2015)
24. Mathe, S., Sminchisescu, C.: Actions in the eye: Dynamic gaze datasets and learnt saliency models for visual recognition. *IEEE Transactions on Pattern Analysis and Machine Intelligence* **37**(7) (July 2015) 1408–1424
25. Stefan Mathe, C.S.: Action from still image dataset and inverse optimal control to learn task specific visual scanpaths. In: *Advances in Neural Information Processing Systems*. (2013)
26. Rudoy, D., Goldman, D.B., Shechtman, E., Zelnic-Manor, L.: Learning video saliency from human gaze using candidate selection. In: The IEEE Conference on Computer Vision and Pattern Recognition (CVPR). (June 2013)
27. Hochreiter, S., Schmidhuber, J.: Long short-term memory. *Neural computation* **9**(8) (1997) 1735–1780
28. Bishop, C.M.: *Mixture density networks*. (1994)
29. Gitman, Y., Erofeev, M., Vatolin, D., Andrey, B., Alexey, F.: Semiautomatic visual-attention modeling and its application to video compression. In: *Image Processing (ICIP), 2014 IEEE International Conference on*. (Oct 2014) 1105–1109
30. Yu, Y., Mann, G.K.I., Gosine, R.G.: An object-based visual attention model for robotic applications. *IEEE Transactions on Systems, Man, and Cybernetics, Part B (Cybernetics)* **40**(5) (Oct 2010) 1398–1412
31. Jiang, M., Xu, J., Zhao, Q.: Saliency in crowd. In: *Computer Vision–ECCV 2014*. Springer (2014) 17–32
32. Li, G., Yu, Y.: Visual saliency based on multiscale deep features. In: The IEEE Conference on Computer Vision and Pattern Recognition (CVPR). (June 2015)
33. Karthikeyan, S., Ngo, T., Eckstein, M., Manjunath, B.: Eye tracking assisted extraction of attentionally important objects from videos. In: *IEEE International Conference on Computer Vision and Pattern Recognition*. (Jun 2015)
34. Borji, A., Sihite, D.N., Itti, L.: Quantitative analysis of human-model agreement in visual saliency modeling: A comparative study. *Image Processing, IEEE Transactions on* **22**(1) (2013) 55–69
35. Judd, T., Ehinger, K., Durand, F., Torralba, A.: Learning to predict where humans look. In: *Computer Vision, 2009 IEEE 12th international conference on*, IEEE (2009) 2106–2113
36. Harel, J., Koch, C., Perona, P.: Graph-based visual saliency. In: *Advances in neural information processing systems*. (2006) 545–552
37. Borji, A., Itti, L.: State-of-the-art in visual attention modeling. *IEEE Transactions on Pattern Analysis and Machine Intelligence* **35**(1) (Jan 2013) 185–207

38. Guo, C., Ma, Q., Zhang, L.: Spatio-temporal saliency detection using phase spectrum of quaternion fourier transform. In: Computer vision and pattern recognition, 2008. cvpr 2008. iee conference on, IEEE (2008) 1–8
39. Zhao, J., Siagian, C., Itti, L.: Fixation bank: Learning to reweight fixation candidates. In: The IEEE Conference on Computer Vision and Pattern Recognition (CVPR). (June 2015)
40. Zhai, Y., Shah, M.: Visual attention detection in video sequences using spatiotemporal cues. In: Proceedings of the 14th annual ACM international conference on Multimedia, ACM (2006) 815–824
41. Huang, X., Shen, C., Boix, X., Zhao, Q.: Salicon: Reducing the semantic gap in saliency prediction by adapting deep neural networks. In: The IEEE International Conference on Computer Vision (ICCV). (December 2015)
42. Cao, C., Liu, X., Yang, Y., Yu, Y., Wang, J., Wang, Z., Huang, Y., Wang, L., Huang, C., Xu, W., Ramanan, D., Huang, T.S.: Look and think twice: Capturing top-down visual attention with feedback convolutional neural networks. In: The IEEE International Conference on Computer Vision (ICCV). (December 2015)
43. Liu, N., Han, J., Zhang, D., Wen, S., Liu, T.: Predicting eye fixations using convolutional neural networks. In: IEEE Conference on Computer Vision and Pattern Recognition, CVPR 2015, Boston, MA, USA, June 7-12, 2015. (2015) 362–370
44. Pan, J., i Nieto, X.G.: End-to-end convolutional network for saliency prediction. CoRR **abs/1507.01422** (2015)
45. Srivastava, N., Mansimov, E., Salakhudinov, R.: Unsupervised learning of video representations using lstms. (2015) 843–852
46. Graves, A.: Generating sequences with recurrent neural networks. CoRR **abs/1308.0850** (2013)
47. Sharma, S., Kiros, R., Salakhutdinov, R.: Action recognition using visual attention. In: ICLR workshops. (2016)
48. Marszałek, M., Laptev, I., Schmid, C.: Actions in context. In: IEEE Conference on Computer Vision & Pattern Recognition. (2009)
49. Soomro, K., Zamir, A.R., Shah, M.: Ucf101: A dataset of 101 human actions classes from videos in the wild. arXiv preprint arXiv:1212.0402 (2012)
50. Judd, T., Durand, F., Torralba, A.: A benchmark of computational models of saliency to predict human fixations. In: MIT Technical Report. (2012)
51. Oliva, A., Torralba, A.: Modeling the shape of the scene: A holistic representation of the spatial envelope. *Int. J. Comput. Vision* **42**(3) (May 2001) 145–175
52. Wang, H., Schmid, C.: Action recognition with improved trajectories. In: Proceedings of the IEEE International Conference on Computer Vision. (2013) 3551–3558